Time domain coupled simulation of machine tool dynamics and cutting forces considering the influences of nonlinear friction characteristics and process damping

Sato, Ryuta
Noguchi, Shin
Hokazono, Taisuke
Nishida, Isamu
Shirase, Keiichi

(Citation)
Precision Engineering,61:103-109

(Issue Date)
2020-01

(Resource Type)
journal article

(Version)
Accepted Manuscript

(URL)
https://hdl.handle.net/20.500.14094/90006675

Title and Authors

Time Domain Coupled Simulation of Machine Tool Dynamics and Cutting Forces considering the Influences of Nonlinear Friction Characteristics and Process Damping

Ryuta SATO, Shin NOGUCHI, Taisuke HOKAZONO, Isamu NISHIDA, and Keiichi SHIRASE

Department of Mechanical Engineering, Kobe University

1-1 Rokko-dai, Nada, Kobe 657-8501, JAPAN

sato@mech.kobe-u.ac.jp

Abstract

A higher machining ability is always required for NC machine tools to achieve higher productivity. The self-oscillated vibration called “chatter” is a well-known and significant problem that increases the metal removal rate. The generation process of the chatter vibration can be described as a relationship between cutting force and machine tool dynamics. The characteristics of machine tool feed drives are influenced by the nonlinear friction characteristics of the linear guides. Hence, the nonlinear friction characteristics are expected to affect the machining ability of machines. The influence of the contact between the cutting edge and the workpiece (i.e., process damping) on to the machining ability has also been investigated. This study tries to clarify the influence of the nonlinear friction characteristics of linear guides and ball screws and process damping onto milling operations. A vertical-type machining center is modeled by a multi-body dynamics model with nonlinear friction models. The influence of process damping onto the machine tool dynamics is modeled as stiffness and damping between the tool and the workpiece based on the evaluated frequency response during the milling operation. A time domain-coupled simulation approach between the machine tool behavior and the cutting forces is performed by using the machine tool dynamics model. The simulation results confirm that the nonlinear frictions influence the cutting forces with an effect to suppress the chatter vibration. Furthermore, the influence of process damping can be evaluated by the proposed measurement method and estimated by a time domain simulation.

Keywords

NC machine tool, milling operation, nonlinear friction characteristics, process damping, chatter, simulation

1. Introduction

The metal-cutting machine tool is one of the important facilities in the manufacturing field. Milling operations are a typical machining operation in machining centers. In milling operations, a higher metal removal rate is required to achieve a higher productivity. However, a self-excited vibration known as chatter becomes a dominant problem in setting a larger cut depth. The chatter is the most dangerous phenomenon because it could grow uncontrollably, causing poor surface finish, tool wear, and breakage [1]. The chatter stability can be analyzed in the frequency domain based on the frequency response function (FRF) [2]. The analysis result can be represented as a visible diagram known as the stability lobe diagram (SLD). The SLD is a very useful tool for finding cutting conditions that can achieve a higher depth of cut.

The chatter stability is directly related with the FRF of machine tools. The FRF can typically be measured by an impulse test using an impulse hummer. Impulse tests are typically performed in the stationary condition (i.e., without any axis movements). However, the SLD during a milling operation is not identical with the analyzed SLD based on the FRF measured in the stationary condition [3].

One of the reasons for the difference is the nonlinear friction characteristics of the linear motion guides and the ball screws of the feed drives. The friction of linear guides and ball screws behaves as nonlinear springs and exhibits higher damping characteristics [4–6]. The nonlinear spring characteristics behave as dampers only in the stationary condition. Tanaka et al. [7] clarified that the nonlinear spring characteristics influence the frequency response of a feed drive. Moreover, the friction of the linear guides and the ball screws have a velocity dependency generally known as the Stribeck curve [8, 9]. Kaneko et al. [10] clarified that both nonlinear spring characteristics and velocity dependency influence the vibration characteristics of a feed drive. Shinagawa and Shamoto [11] clarified that the friction force of the linear guides exhibits higher chatter stabilities.

The influence of the contact between the tool tip and the workpiece surface can be a reason of the FRF change. This phenomenon is generally called process damping [12–14]. Altintas et al. [12] tried to identify the process damping parameters that can be applied to the SLD analysis. Budak and Tunk [13, 14] proposed an identification method for process damping parameters and investigated the influence of cutting conditions and tool geometry. Grossi et al. [15] also investigated the influence of the cutting speed onto the FRFs under operating conditions.

As mentioned earlier, both nonlinear friction characteristics and process damping influence the FRFs of the machine tools. However, no research work has yet investigated the influence of both important characteristics together. Suzuki et al. [16] proposed an inverse identification method for the machine tool dynamic parameters based on the measured chatter vibrations. However, the identified results can only represent the total equivalent parameters and cannot be divided to the influence of each factor.

This study tries to clarify the influence of the nonlinear friction characteristics of linear guides and ball screws and process damping on milling operations. A vertical-type machining center is modeled herein by a multi-body dynamics model with nonlinear friction models. The influence of the process damping onto the machine tool dynamics is also modeled as stiffness and damping between the tool and the workpiece based on the evaluated frequency response during the milling operation. A time domain-coupled simulation approach between the machine tool behavior and the cutting forces is performed using the machine tool dynamics model to evaluate the influence of nonlinear frictions and process damping.

2. Machine Tool Model and Coupled Simulation Method

A vertical-type machine tool was used in the experiment. This machine had X- and Y-axes in the table and a Z-axis in the spindle. All feed drive systems were driven by a ball screw and an AC servo motor. The motion of each axis was guided by linear ball guides. Each feed drive system consisted of the feed drive mechanism and the control system. In the control system, the position controller was a proportional (P) controller, while the velocity controller was a proportional-integral (PI) controller. The position control loop was a semi-closed control based on the feedback rotation angle of the motor. Figure 1(a) shows the machine tool dynamic model [17].

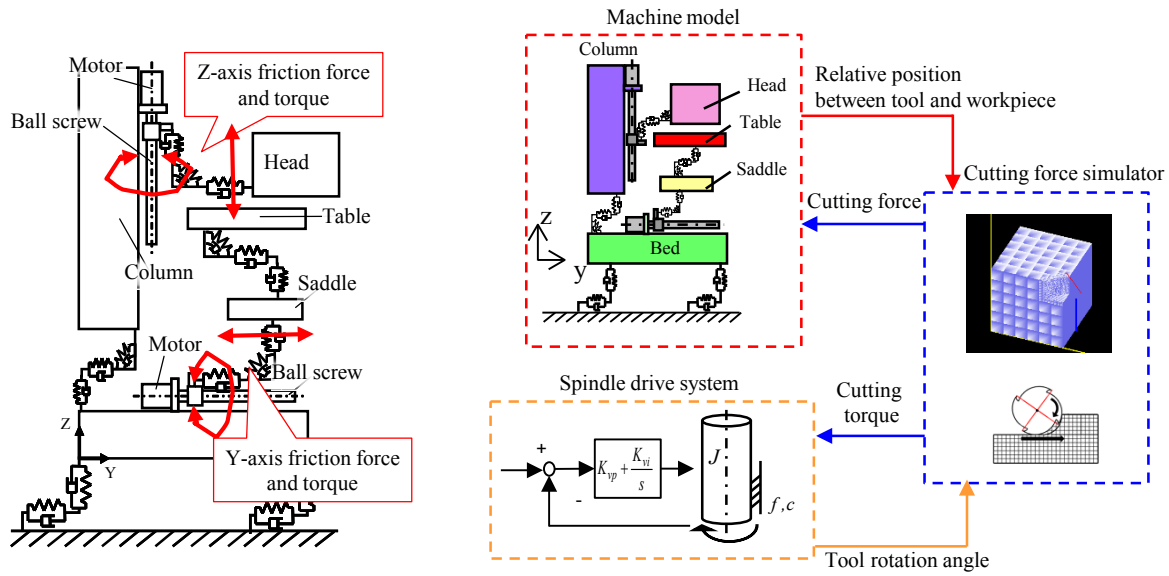

(a) Vibration model of a machine tool

(b) Coupled simulation method between machine tool dynamics and cutting forces

Figure 1. Machine tool model and coupled simulation method between machine tool dynamics and cutting forces.

The machine tool structure in this model was composed of five elements (i.e., head, column, saddle, table, and bed). These five elements had 3 degrees of freedom (DOF) for each translation and rotation. The feed

drive mechanism models to consider friction were installed between the saddle and the table, the saddle and the bed, and the column and the head. The feed drive mechanism models were modeled as 2 DOF, which considered the rotation and the liner motion of the driven body by the motor and the ball screw. The machine tool model had a total of 33 DOF. The X-, Y-, and Z-axial directional stiffness and dampers were installed between the bed and the ground to express the machine bed support.

The undeformed chip thickness in the general instantaneous rigid force model for the cutting force simulation [18] is defined by a geometrical approximate equation. However, the relative displacement changing between the tool and the workpiece derived from the dynamic behaviors is impossible to consider. In this study, a cutting simulator referring voxel model was applied for the cutting force simulation [19]. The workpiece in this simulator was represented by the voxel model. The undeformed chip thickness was discretely calculated from the number of voxels removed by the cutting edge for each instantaneous minute tool rotational angle.

In this method, the number of removal voxels is changed if the relative displacement between the tool and the workpiece is changed by the machine dynamic behavior. Therefore, the influence of the machine dynamic behavior on the cutting force was observed. In addition, the voxel remains in the following calculation steps if it is not removed for each instantaneous minute rotational angle. In other words, the workpiece shape after passing the tool edge is reflected in the cutting force simulation by the next cutting edge.

Figure 1(b) describes the coupled simulation method between the machine tool behavior and the cutting force [20, 21]. The relative displacement of the tool to the workpiece was calculated by the machine structure and feed drive system model. The tool rotational angle was calculated by the spindle drive system model. The cutting-edge coordinate in the three-dimensional space was calculated from the relative displacement and tool rotational angle. The undeformed chip thickness was then calculated by the voxel simulator from this cutting edge coordinate. Finally, the cutting force and the cutting torque were calculated. The calculated cutting force and torque were applied into the machine structure and feed drive system model and the spindle drive system model. The next time step relative displacement of the tool and the work piece and the tool rotational angle was then calculated. A coupled simulation between the machine tool behavior and the cutting force was subsequently realized by repeating the abovementioned steps. The moment by cutting force was applied into the machine table and the head in addition to the disturbance force in the three translational directions because the point of application of the cutting force was different from the point of gravity of the machine table and the head when applying cutting force into the machine structure and feed drive system model. The coupled simulation method was already confirmed to simulate the chatter vibration generation.

3. Friction Model

The friction characteristics of the ball screws and the linear ball guides had both position and velocity dependencies [5–8]. Although various modeling strategies based on the physical phenomena exist [22], the friction characteristics of the ball screws and the linear ball guides can still be simply modeled as Equations (1) and (2), respectively, based on the results from previous research works [10, 23].

$$f_b = \left\{f_{cb} + \left(C_b + C_{vb}e^{-a_{vb}|\dot{\theta}|}\right)\dot{\theta}\right\}(2\tanh\left(a_{hb}\theta'\right) - 1)\mathrm{sgn}(\dot{\theta}) \quad (1)$$

$$f_t = \left\{f_{ct} + \left(C_t + C_{vt}e^{-a_{vt}|\dot{x}|}\right)\dot{x}\right\}(2\tanh\left(a_{ht}x'\right) - 1)\mathrm{sgn}(\dot{x}) \quad (2)$$

Equation (1) represents the rotational friction torque: friction torque of the ball screw and the bearings. The equation consists of velocity dependence and displacement dependence parts. In the velocity dependence part, f_{cb} is Coulomb's friction torque [Nm], while C_b is the viscous coefficient [Nm/(rad/s)]. C_{vb} and a_{vb} are the parameters for the nonlinear velocity dependency. In the position dependent part, θ' is the angular displacement from the motion direction reversal points [rad]. a_{hb} is the inclination parameter representing the relationship between angular displacement and friction torque. A larger a_{hb} increases the friction torque faster. Equation (2) also represents the translational friction force: friction force of the linear ball guides and telescopic covers. The parameters of the equation are defined as similar to those of the model for the rotational friction torque. The models were installed into the machine tool model shown in Figure 1(a).

The values of the inclination parameters a_{hb} and a_{ht} were determined to keep the friction constant at around 300 μrad and 300 μm based on the previous research works [6, 8]. The amount of friction torque and force were determined by the velocity dependence part in the equations. The values for the velocity dependency were determined by matching the measured relationships between the angular velocity of the motor and the motor torque. The motor torque was recorded during the constant feed motion speed with various velocities. The average values of the torque were plotted as a function of the rotational velocity. The motor torque during the constant speed included all of the frictions in the mechanism. The parameters of the rotational and translational friction models herein were determined assuming that the torque influence around the motor shaft by each friction was equivalent. The influence of the rotational and translational frictions is expected to not be equivalent because it depends on the mechanism design. The motor torque and the rotational velocity of the motor can be recorded using the monitoring function of the NC controller.

Figure 2 shows the measured and simulated friction characteristics of the Y-axis for an example. Figure 2(a) depicts the relationships between the displacement of the table and the motor torque. The motor torque during the circular motion with a radius of 0.2 mm and a feed rate of 5 mm/min was measured. The torque was represented as the function of the displacement. A motor torque simulation was performed with the

circular motion of the same condition. Figure 2(b) shows the measured and simulated relationships between the angular velocity and the motor torque. According to Figure 2(a), although the nonlinear spring can be adequately simulated, the simulated torque was smaller than the measured one. The friction torque was determined by the velocity dependence part of the model. According to Figure 2(b), the friction torque became minimum around 5 or 10 rad/s. These velocities were around 600 mm/min. The velocity applied for the measurement of the nonlinear spring characteristics was smaller than the velocity range represented in Figure 2(b). Although the friction was expected to become larger in a lower velocity range, the friction model shown in Equations (1) and (2) cannot express the phenomena. The proposed friction model was adopted to avoid the friction model with too many parameters to achieve the purpose of this study. Table 1 lists the determined values for the friction models.

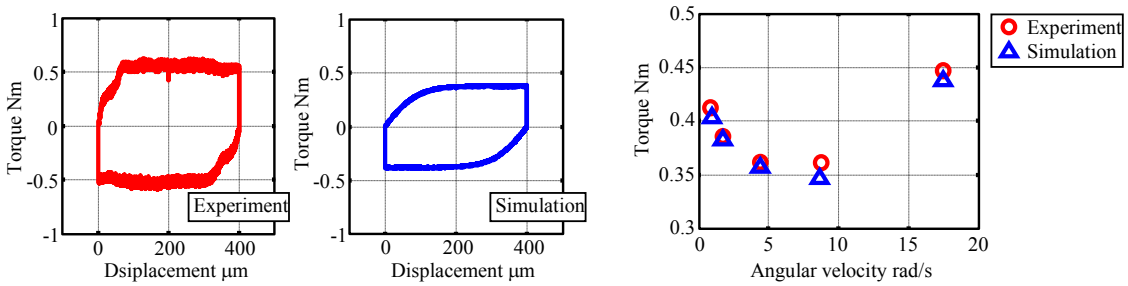

(a) Non-linear spring characteristics of friction (b) Velocity dependency of friction

Figure 2. Comparison of the measured and simulated friction characteristics of the Y-axis.

Table 1. Determined parameters for the friction models.

(a) Rotational friction torque model

Parameter	X-axis	Y-axis	Z-axis
f_{cb}	0.188 Nm	0.113 Nm	0.046 Nm
C_b	3.2×10^{-3} Nm/(rad/s)	3.2×10^{-3} Nm/(rad/s)	1.3×10^{-3} Nm/(rad/s)
C_{vb}	0.03	0.25	0.35
a_{vb}	2	2	2.75
a_{hb}	1.15×10^{4}	1.15×10^{4}	1.15×10^{4}

(b) Translational friction force model

Parameter	X-axis	Y-axis	Z-axis
f_{ct}	98.6 N	99.2 N	17.95 N
C_t	856.2 N/(m/s)	426.7 N/(m/s)	189.3 N/(m/s)
C_{vt}	3000	6000	6000
a_{vt}	500	500	800
a_{ht}	1.15×10^{4}	1.15×10^{4}	1.15×10^{4}

4. Influence of the Nonlinear Friction on the Frequency Response

The nonlinear friction characteristics provide a damping effect [4, 7, 8, 10]. The nonlinear spring characteristics only showed effect during the stationary condition without feed motion because the characteristics can exist around several hundred micrometers around the motion direction changing points. The velocity dependency of the friction can also influence the difference of the frequency response because of the difference of the velocity range between the stationary and moving conditions.

Figure 3(a) shows the measured FRFs along the Y-axis direction. The measurement tests were performed with two conditions: stationary and moving. The feed rate of the axis for the stationary condition test was set to 0. Meanwhile, the Y-axis feed rate for the moving conditions was set to 420 mm/min. An accelerometer was attached on the worktable, and the table was excited to +Y direction by an impulse hammer. For the measurement during the feed motion, the table was oscillated to the +Y direction when the Y-axis was moving to the same direction. Figure 3(a) shows a large resonant vibration around 50 Hz. The amplitude of the vibration became much smaller when the axis did not move. Figure 3(c) illustrates the vibration mode at the resonance frequency around 50 Hz. The dominant mode is the bending mode between the bed and the column around the X-axis direction. The saddle, where the axial position was controlled by the Y-axis feed drive was vibrating along the Y-axis at the same time. The saddle vibration was influenced by the frictions of the Y-axis feed drive mechanism.

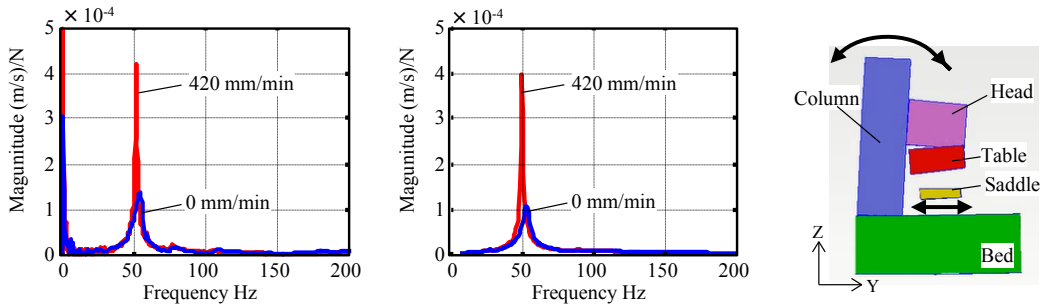

(a) Measured frequency responses (b) Simulated frequency responses (c) Vibration mode

Figure 3. Comparison of the measured and simulated frequency responses along the Y-axis direction in case of stationary and moving conditions.

Figure 3(b) shows the simulated FRFs. In the simulations, the impulse force was applied to the table along the Y-axis direction. The Y-axis acceleration of the table was then simulated similar to the measurements. The stiffness and damping parameters of the model were identified based on the measured frequency response in the moving condition. According to Figure 3(b), the large resonance vibration around 50 Hz can also be reduced when the axis does not move similar to that in the measured results. The simulated FRF without the friction models was identical to that in the moving condition with the friction models.

The results showed that the proposed friction model can express the influence of the friction onto the vibration characteristics of the whole machine tool structure. Furthermore, the friction of the ball screws and the linear guides significantly influenced the frequency characteristics of the machine tools.

5. Evaluation of Process Damping and Contacting Stiffness

Many studies on process damping have been conducted to date [12–16]. However, directly evaluating the influence of the contact between the tool tip and the workpiece onto the frequency characteristics of the machine tools is difficult. Therefore, an evaluation method for the frequency response during the cutting operation was proposed herein.

Figure 4 describes the measurement test method. The milling operation is an intermittent cutting process; hence, the machine tool is oscillated at each intermittent contact between the tool tip and the workpiece. Accordingly, the boring process that can be a continuous cutting process was adopted to avoid the oscillation by the cutting force. The tool was an insert tip-type milling tool with five teeth, which is similar with the tool used in the cutting test, and has diameter of 50 mm. For the boring test, four insert tips were detached from the tool to be used as a boring tool. A hole with 45 mm diameter was prepared for the material (JIS S45C carbon steel block). As a result, the radial depth of cut became 2.5 mm. The rotational speed of the spindle and the feed rate of the Z-axis were 180 rpm and 18 mm/min, respectively. The resulting axial depth of cut was 0.1 mm.

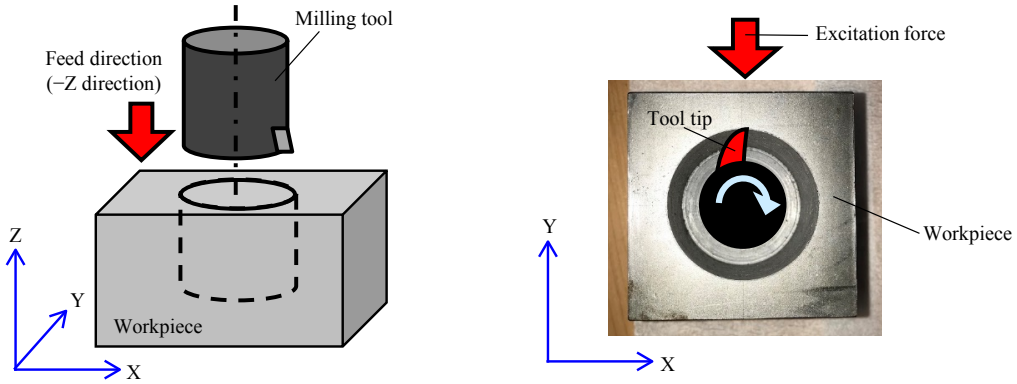

(a) Boring operation (b) Excitation timing

Figure 4. Boring test to evaluate the influence of the contact between the tool tip and the workpiece.

The impulse excitation force was applied as an impulse torque command to the Y-axis motor (Figure 5). In the developed system, the input timing of the impulse torque command can be controlled as a function of the rotational angle of the spindle. The impulse torque command was applied to the −Y direction at the timing of the tool tip comings to the +Y direction (Figure 4(b)). The axial acceleration along the Y-axis

was measured by an accelerometer attached to the table. Both X- and Y-axes did not move during the boring operation. The FRF can be evaluated from the input torque command and the measured acceleration. The impulse torque can be calibrated to the impulse force to the table by comparing the amplitude of the excited vibration.

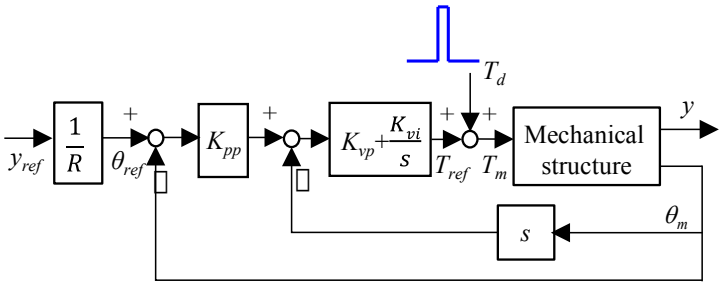

Figure 5. Simplified block diagram of the feed drive system with the impulse torque command.

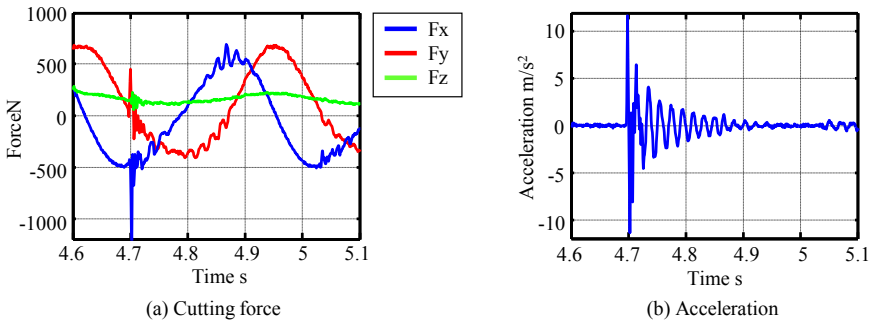

Figure 6. Measured cutting force and acceleration during the boring operation with the impulse torque input.

Figure 6 shows the measured cutting forces and acceleration of the table. The cutting forces were measured by a dynamometer (KISTLER 9257B). The X-axis cutting force *Fx* and the Y-axis cutting force *Fy* became a simple sinusoidal wave in the boring operation. The X-axis cutting force *Fx* became maximum when the cutting edge was located at the +Y direction. Figure 6(a) illustrates that spike-like cutting fore changes can be observed around 4.7 s. These changes came from the impulse torque input for excitation. The residual vibration can clearly be observed around between 4.7 s and 4.9 s (Figure 6(b)). The FRF was evaluated based on the measured acceleration.

Figure 7(a) shows the measured FRFs. The measurement tests were performed both with and without cutting. Both FRFs were measured by the method using the impulse torque input. The X- and Y-axis feed drives did not move during the measurement. According to the figure, the FRF was changed during the cutting process. The resonance frequency became 2 Hz higher. Moreover, the amplitude became 62.7%

during the cutting. The changing of the frequency and the amplitude came from the contact between the tool tip and the workpiece.

The stiffness and damping were introduced between the head and the table of the machine tool model in both X- and Y-directions (Figure 7(c)) to evaluate the equivalent stiffness and damping by the contacting effect. The stiffness and the damping were identified by matching the differences of the measured FRFs of with and without cutting. As a result, the stiffness and the damping became 2.50 N/μm and 3.35 kN/(m/s), respectively. Figure 7(b) shows the simulated FRFs using the identified values.

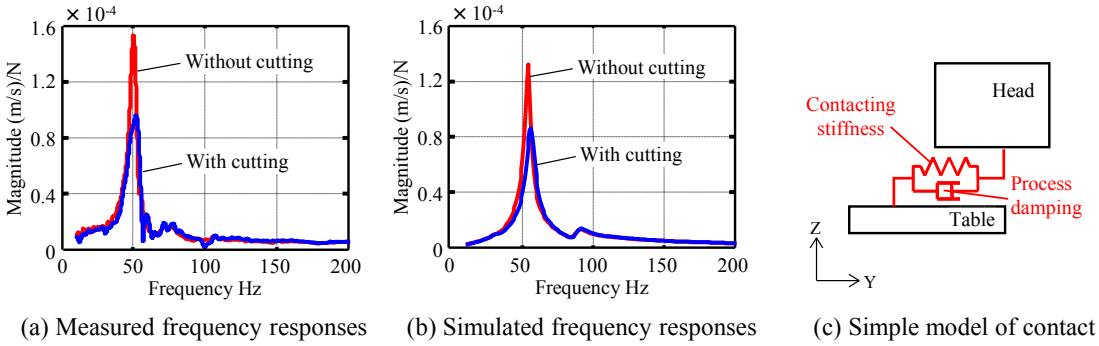

(a) Measured frequency responses (b) Simulated frequency responses (c) Simple model of contact

Figure 7. Influence of the contact between the tool tip and the workpiece onto the frequency characteristics.

The stiffness and the damping caused by the contact were expected to depend on the cutting speed, cut depth, exciting force, workpiece material, lubricant condition, rake and clearance angles of the tool, and so on. However, in this study, the identified values from the FRFs shown in Figure 7 were used for the coupled simulation. We will try to clarify the influence of various factors on the contacting effect.

6. Cutting Test and Simulation Results

The milling test and simulations were performed to investigate the influence of the nonlinear friction characteristics and process damping in the milling operation. The tool and the material for the milling test are the same as those used for the evaluation of process damping and contacting stiffness. Figure 8 shows the experimental set-up. The feed direction is the –X direction without any Y-axis motion. The cutting force during the test was measured by a dynamometer. Table 2 presents the cutting condition. Figure 9 shows the measured cutting forces. The condition in Table 1 is the stable cutting condition.

Coupled simulations were performed with three kinds of combinations: without both nonlinear friction and contacting effect, with nonlinear friction and without contacting effect, and with both the nonlinear friction and the contacting effect. Figure 10 shows the simulated cutting forces without both the nonlinear friction

and the contacting effect. The chatter vibration is yielded at approximately 50 Hz although the tooth passing frequency is 70 Hz. As the result, the cutting force waveforms are disturbed in the case of occurrence of chatter vibrations. According to the result, chatter vibration started around 1 s even though there is no chatter in the experiment. Figure 11 shows the results with only the nonlinear friction characteristics of the ball screws and the linear guides. The starting time of the chatter vibration was later than that in Figure 10. The result showed that the nonlinear friction characteristics had an effect in suppressing the chatter vibration. The simulation result with both the nonlinear friction characteristics and the contacting effect is shown in Figure 12. The chatter vibration did not exist until 2 s in the result similar to that in the experiment. The chatter vibration started to generate after 2 s in the simulation, a shown in Figure 12. On the other hand, the chatter vibration did not exist in the experiment. It is expected that the actual process damping changes during the cutting operation due to the direction of tool tip and cutting depth, although the process damping is modeled as a linear viscous damper in this study. We will try to investigate the changing of process damping during the cutting operations and improve the model based on the investigation.

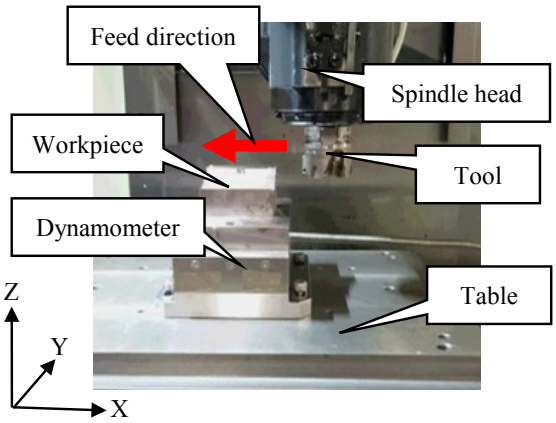

Figure 8. Experimental set-up for the milling test.

Table 2. Cutting condition.

Workpiece material	JIS S45C
Tool type	□ 50 face mill
Helix angle	14°
Number of teeth	5
Axial depth of cut	5 mm
Radial depth of cut	5 mm
Spindle speed	840 rpm
Cutting direction	Down cut

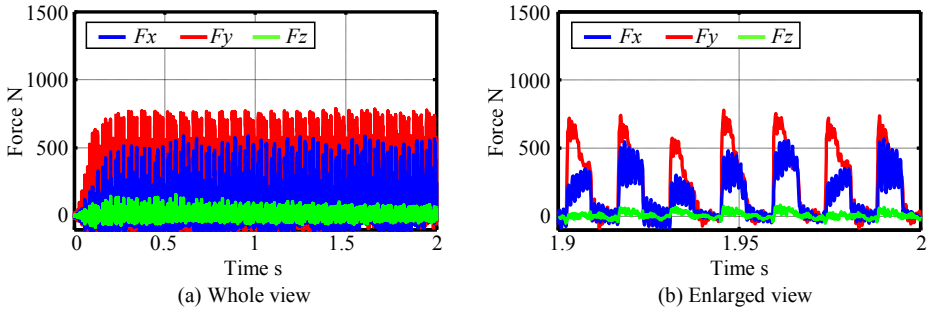

Figure 9. Measured cutting force.

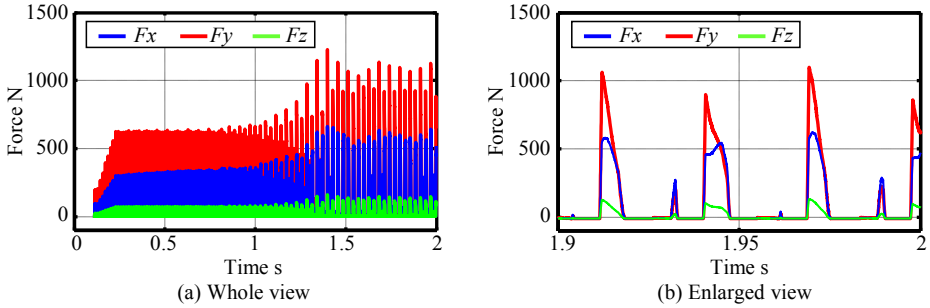

Figure 10. Simulated cutting force without both nonlinear friction and contacting effect.

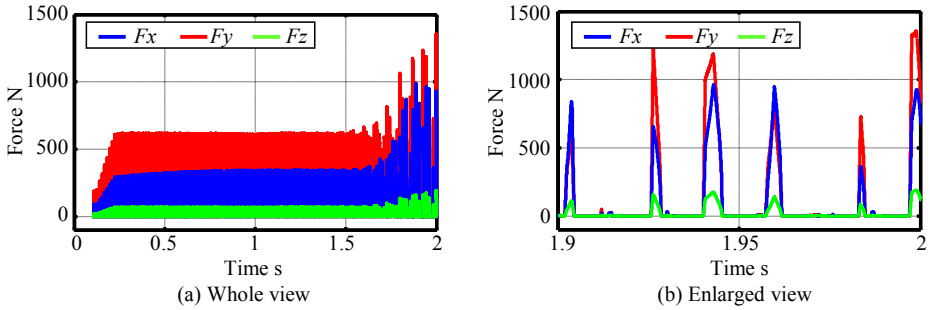

Figure 11. Simulated cutting force only with the nonlinear friction.

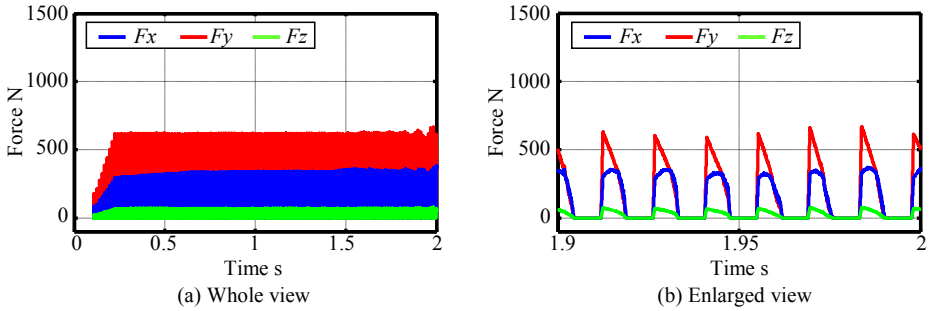

Figure 12. Simulated cutting force with both nonlinear friction and contacting effect.

As mentioned earlier, although we have to conduct a deeper investigation, the FRF of the machine tool during the cutting operation can adequately be evaluated by the impulse torque command input, and both nonlinear friction characteristics and contacting effect have a significant role in suppressing the chatter vibration in the milling process. According to Figure 3(a), the magnitude of the vibration changes from 4.2×10^{-4} (m/s)/N to 1.6×10^{-4} (m/s)/N due to the nonlinear friction characteristics. This effect is 4.3 times larger than the influence of the process damping that decreases the vibration from 1.6×10^{-4} (m/s)/N to 1.0×10^{-4} (m/s)/N, as shown in Figure 7(a). However, it is difficult to conclude that the contribution of the nonlinear friction characteristics is always larger than the contribution of the process damping, because it is expected that the influences depend on many factors such as the vibration mode. We will try to clarify the influences of the nonlinear friction characteristics and process damping onto the vibration characteristics.

7. Conclusions

This study tried to clarify the influence of the nonlinear friction characteristics of linear guides and ball screws and process damping on milling operations. A vertical-type machining center was modeled by a multi-body dynamics model with nonlinear friction models. The influence of process damping on the machine tool dynamics was modeled as stiffness and damping between the tool and the workpiece based on the evaluated frequency response during the milling operation. A time domain-coupled simulation approach between the machine tool behavior and cutting forces was performed to evaluate the influence of the nonlinear frictions and process damping. The conclusions can be summarized as follows:

1) The proposed friction model can express the influence of friction onto the vibration characteristics of the whole machine tool structure.
2) The friction of ball screws and linear guides significantly influence the frequency characteristics of the machine tools.
3) Both nonlinear friction characteristics and contacting effect between the tool tip and the workpiece have a significant role in suppressing the chatter vibration in the milling process.
4) The FRF of the machine tool during the cutting operation can adequately be evaluated by the impulse torque command input.

The simulation and evaluation techniques used in this study can be effective in clarifying the dynamic behavior of machine tools during the machining process. We will try to clarify the influence of various

factors to the process damping effect and will try to develop a more detailed model for the process damping effect to investigate the dynamic behaviors during the machining process.

Acknowledgment

This study was supported by Osawa Scientific Studies Grants Foundation, JSPE KAKENHI Grant Numbers JP18H01350 and JP17H03158.

References

[1] G. Quintana, and J. Ciurana, Chatter in Machining Process: A Review, International Journal of Machine Tools & Manufacture, 51 (2011) 363–376.

[2] Y. Altintaş, and E. Budak, Analytical Prediction of Stability Lobes in Milling, CIRP Annals, 44 (1995) 357–362.

[3] N. Grossi, A. Scippa, L. Sallese, R. Sato, and G. Campatelli, Spindle Speed Ramp-Up Test: A Novel Experimental Approach for Chatter Stability Detection, International Journal of Machine Tools & Manufacture, 89 (2015) 221–230.

[4] P.R. Dahl, Solid Friction Damping of Mechanical Vibrations, AIAA Journal, 14 (1976) 1675–1682.

[5] J.F. Cuttino, T.A. Dow, and B.F. Knight, Analytical and Experimental Identification of Nonlinearities in a Single-Nut, Preloaded Ball Screw, Transactions of the ASME, Journal of Mechanical Design, 119 (1997) 15–19.

[6] S. Fukada, B. Fang, and A. Shigeno, Experimental Analysis and Simulation of Nonlinear Microscopic Behavior of Ball Screw Mechanism for Ultra-precision Positioning, Precision Engineering, 35 (2011) 650–668.

[7] T. Tanaka, K. Ikeda, J. Otsuka, I. Masuda, and T. Oiwa, Influence of Rolling Friction in Linear Ball Guideway on Positioning Accuracy, International Journal of Precision Engineering & Manufacturing, 8 (2007) 85–89.

[8] R. Sato, M. Tsutsumi, and D. Imaki, Experimental Evaluation on the Friction Characteristics of Linear Ball Guides, Transactions of the Japan Society of Mechanical Engineers, Series C, 73, 734 (2007) 2811–2819 (in Japanese).

[9] M. Woydt, and R. Wäsche, The History of the Stribeck Curve and Ball Bearing Steels: The Role of Adolf Martens, Wear, 268 (2010) 1542–1546.

[10] S. Kaneko, R. Sato, and M. Tsutsumi, Mathematical Model of Linear Motor Stage with Non-Linear Friction Characteristics, Journal of Advanced Mechanical Design, Systems, & Manufacturing, 2 (2008) 675–684.

[11] M. Shinagawa, and E. Shamoto, Prediction of Chatter Stability of Machine Tool with Consideration of Friction Damping in Guide (Development of Basic Model and Investigation on Effects of Friction and Stiffness), Transactions of the Japan Society of Mechanical Engineers, Series C, 78, 787 (2012) 1013–1025 (in Japanese).

[12] Y. Altintas, M. Eynian, and H. Onozuka, Identification of Dynamic Cutting Force Coefficients and Chatter Stability with Process Damping, CIRP Annals, 57 (2008) 371–374.

[13] E. Budak, and L.T. Tunc, Identification and Modeling of Process Damping in Turning and Milling Using a New Approach, CIRP Annals, 59 (2010) 403–408.

[14] L.T. Tunç, and E. Budak, Effect of Cutting Conditions and Tool Geometry on Process Damping in Machining, International Journal of Machine Tools & Manufacture, 57 (2012) 10–19.

[15] N. Grossi, L. Sallese, A. Scippa, and G. Campatelli, Improved Experimental–Analytical Approach to Compute Speed-Varying Tool-Tip FRF, Precision Engineering, 48 (2017) 114–122.

[16] N. Suzuki, Y. Kurata, T. Kato, R. Hino, and E. Shamoto, Identification of Transfer Function by Inverse Analysis of Self-Excited Chatter Vibration in Milling Operations, Precision Engineering, 36 (2012) 568–575.

[17] R. Sato, G. Tashiro, and K. Shirase, Analysis of the Coupled Vibration between Feed Drive Systems and Machine Tool Structure, International Journal of Automation Technology, 9 (2015) 689–697.

[18] Y. Altintas, Manufacturing Automation, Cambridge University Press (2000).

[19] T. Hasegawa, R. Sato, and K. Shirase, Cutting Force Simulation Referring Workpiece Voxel Model for End-Milling Operation and Adaptive Control Based on Prediction Cutting Force, Journal of the Japan Society for Precision Engineering, 82 (2016) 467–472 (in Japanese).

[20] S. Noguchi, R. Sato, I. Nishida, and K. Shirase, Coupled Simulation between Machine Tool Behavior and Cutting Force Using Voxel Simulator, Proceedings of the 9th International Conference on Leading Edge Manufacturing in 21st Century (LEM21), (2017) No. 044.

[21] S. Noguchi, I. Nishida, R. Sato, and K. Shirase, Time Domain Coupled Simulation of Machine Tool Dynamic Behavior and Cutting Force based on Voxel Simulator of Machining Operation, Transactions of the Japan Society of Mechanical Engineers, 83, 856 (2017) No.17-00254 (in Japanese).

[22] C. Canudas de Wit, H. Olsson, K.J. Astrom, and P. Lischinsky, A New Model for Control of Systems with Friction, IEEE Transactions on Automatic Control, 40 (1995) 419–425.

[23] R. Sato, Generation Mechanism of Quadrant Glitches and Compensation for It in Feed Drive Systems of NC Machine Tools, International Journal of Automation Technology, 6 (2012) 154–162.